Photoelectron spectroscopy of color centers in negatively charged cesium iodide nanocrystals

Harry W. Sarkas,[a] Linda H. Kidder, and Kit H. Bowen[b]
Department of Chemistry, Johns Hopkins University, Baltimore, Maryland 21218

(Received 1 July 1994; accepted 19 July 1994)

We present the photoelectron spectra of negatively charged cesium iodide nanocrystals recorded using 2.540 eV photons. The species examined were produced using an inert gas condensation cluster ion source, and they ranged in size from $(CsI)^-_{n=13}$ to nanocrystal anions comprised of 330 atoms. Nanocrystals showing two distinct types of photoemission behavior were observed. For $(CsI)^-_{n=13}$ and $(CsI)^-_{n=36-165}$, a plot of cluster anion photodetachment threshold energies vs $n^{-1/3}$ gives a straight line extrapolating (at $n^{-1/3}=0$, i.e., $n=\infty$) to 2.2 eV, the photoelectric threshold energy for F centers in bulk cesium iodide. The linear extrapolation of the cluster anion data to the corresponding bulk property implies that the electron localization in these gas-phase nanocrystals is qualitatively similar to that of F centers in extended alkali halide crystals. These negatively charged cesium iodide nanocrystals are thus shown to support embryonic forms of F centers, which mature with increasing cluster size toward condensed phase impurity centers. Under an alternative set of source conditions, nanocrystals were produced which showed significantly lower photodetachment thresholds than the aforementioned F-center cluster anions. For these species, containing 83–131 atoms, a plot of their cluster anion photodetachment threshold energies versus $n^{-1/3}$ gives a straight line which extrapolates to 1.4 eV. This value is in accord with the expected photoelectric threshold energy for F' centers in bulk cesium iodide, i.e., color centers with two excess electrons in a single defect site. These nanocrystals are interpreted to be the embryonic F'-center containing species, $Cs(CsI)^-_{n=41-65}$. © *1995 American Institute of Physics.*

I. INTRODUCTION

Alkali halide clusters have been studied extensively due in part to the simple nature of the ionic bonding exhibited in these systems.[1,2] The most thoroughly studied class of alkali halide clusters are the fully ionic clusters, i.e., species composed entirely of M^+ and X^- ions, such as $(MX)_n$, $M^+(MX)_n$, and $X^-(MX)_n$.[3,4] The results of mass spectrometric abundance studies on charged alkali halide clusters,[5–13] together with more recent reactivity studies[14] and ultraviolet absorption studies,[15] indicate that fully ionic alkali halide clusters have a strong tendency to take on cuboidal nanocrystal arrangements that resemble portions of bulk simple-cubic, rocksalt lattices. The study of these species has made a substantial contribution to our understanding of how crystalline structures emerge at small cluster sizes, and accordingly are being used as model systems for examining other structural aspects of nanocrystals.[16]

Alkali halide clusters possessing excess electrons not associated with halogen anions constitute another class of alkali halide clusters. The interaction of excess electrons with alkali halide nanocrystals has been the subject of several theoretical studies.[17–21] Calculations by Landman, Scharf, and Jortner first considered the interaction of excess electrons with sodium halide clusters at finite temperatures.[17] Several possible outcomes for excess electron localization were predicted, including the localization of electrons in halogen anion vacancies, analogous to F-center localization in bulk alkali halide crystals.[22–25] The results of ionization potential measurements[26] and optical absorption experiments[27] on neutral excess electron alkali halide clusters ($n\leqslant 30$) by Whetten and co-workers were found to be supportive of these theoretical predictions.

Negatively charged alkali halide clusters having excess electrons not associated with halogen anions are either stoichiometric cluster anions, $(MX)^-_n$, with single excess electrons, or excess metal cluster anions, $M_m(MX)^-_n$, with multiple excess electrons. Such alkali halide cluster anions have been investigated via negative ion photoelectron spectroscopy in experiments by Miller and Lineberger[28] on $(NaF)^-_{n\leqslant 12}$ and $Na(NaF)^-_{n\leqslant 12}$; by Bloomfield and Smalley[29] on $(KI)^-_{n\leqslant 13}$ and $K_{1,2}(KI)^-_{n\leqslant 13}$; and by Bloomfield and co-workers[30–33] on $(NaCl)^-_{n\leqslant 13,22}$ and $Na(NaCl)^-_{n\leqslant 21}$. From the photoelectron spectra and accompanying calculations, $(KI)^-_{13}$ and $(NaCl)^-_{13}$ were interpreted as being F-center species having $3\times3\times3$ cubic arrangements (with single excess electrons occupying corner anion vacancies), while $(NaCl)^-_{22}$ was likewise proposed to be a corner F-center species with a $3\times3\times5$ structure. For $K_{1,2}(KI)^-_{n\leqslant 13}$ and $Na(NaCl)^-_{n\leqslant 21}$, it was proposed that their multiple excess electrons could be localized, depending on the specific cluster anion size, separately in different F-center sites, or together as spin pairs in M^- sites analogous to bipolarons in bulk crystals. In addition, for certain small $Na(NaCl)^-_n$ cluster anions, it was proposed that two excess electrons could be localized together in single anion vacancies as F' centers.[33]

Here, we present the visible photoelectron spectra of negatively charged cesium iodide nanocrystals containing between 26 and 330 atoms. The present study is complimentary to the aforementioned studies on smaller excess electron alkali halide cluster anions, examining a cluster anion size

[a]Present address: US Naval Research Laboratory, Washington, DC 20375.
[b]Author to whom all correspondence should be addressed.

range extending to substantially larger sizes than those previously investigated. The approach taken here allows different types of electron binding behavior in these nanocrystals to be identified, tracked as functions of cluster size, and subsequently correlated with excess electron localization mechanisms found in the corresponding bulk crystals. The correlations with bulk observed in this work provide evidence for the existence of two types of embryonic color centers in negatively charged CsI nanocrystals, i.e., F centers (one excess electron trapped in an anion vacancy) and F' centers (two excess electrons in a single vacancy).

II. EXPERIMENTAL METHOD

Negative ion photoelectron spectroscopy is conducted by crossing a mass-selected beam of negative ions with a fixed-frequency photon beam and energy analyzing the resultant photodetached electrons. Our negative ion photoelectron spectrometer has been described previously.[34] Anions generated in an appropriate ion source (see below) are accelerated, collimated, and transported via a series of ion optical components, before being mass selected with an $\mathbf{E}\times\mathbf{B}$ Wien velocity filter. The mass-selected ion beam is then focused into a field-free, collision-free interaction region, where it is crossed with the intracavity photon beam of an argon ion laser operated at 488 nm (2.540 eV) and circulating powers of $\sim$100 W. A small solid angle of the resulting photodetached electrons is accepted into the input optics of a magnetically shielded, hemispherical electron energy analyzer, where the electrons are energy analyzed and counted. Photoelectron spectra were calibrated by recording spectra of O^- generated in a secondary beam, introduced only when the main beam was not in operation.

Although unit cluster anion mass selectivity was not achieved over much of the cluster anion mass distribution due to the large cluster anion masses involved (3380–42 900 amu), the accuracy of the mass calibrations was easily sufficient to determine the cluster sizes of the largest cesium iodide cluster anions to within a few CsI units. This was facilitated by the fact that both Cs and I occur naturally as single isotopes. In addition, the spectral shifts between the photoelectron spectra of adjacent-sized cesium iodide nanocrystal anions of a given type are rather small, so that contributions from adjacent cluster anions do not significantly alter the spectrum of a given cluster anion.

III. CESIUM IODIDE CLUSTER ANION GENERATION AND INITIAL CHARACTERIZATION

Beams of cesium iodide cluster anions with masses extending well beyond 50 000 amu were generated using our inert gas condensation cluster ion source.[35] In the past, inert gas condensation has been employed by Martin[11,36,37] and by Sattler, Recknagel, and co-workers[12,38] to generate beams of neutral and cationic alkali halide clusters. In our ion source, an oven evaporates the material of interest into a cell containing cool helium gas. The vapor supersaturates in this cool environment and nucleates, forming nanometer-sized clusters. The condensation cell is coupled to high vacuum by a small aperture, resulting in a helium flow which entrains the nanoclusters and transports them into vacuum via a rather weak supersonic expansion. A negatively biased hot thoriated iridium filament located on the high vacuum side of the condensation cell aperture serves as a thermionic cathode, creating a discharge in the environment of the expanding jet where negative ions are generated. The resulting plasma is confined by a predominantly axial magnetic field created via six cylindrical rare earth magnets.

Typical source conditions in these experiments included cathode bias voltages of -60 V with filament emission currents of 2–4 mA. Plasma environments similar to those in this ion source are known to possess high densities (10^{11}–10^{13} cm^{-3}) of very low energy electrons in addition to the primary electrons emitted directly from the cathode.[39] The electron energy distributions within such plasmas have been examined via probe measurements[39,40] which show that even under widely varying conditions, the majority of electrons are low energy thermal electrons, with characteristic temperatures of a few electron volts. In addition, it was discovered that the number of thermal electrons in such discharges often exceeds the number of primary electrons by a factor of 10^3. These findings suggest that negative ion production in the inert gas condensation ion source most likely proceeds by the attachment of thermal electrons in the source plasma to neutral clusters formed in the condensation cell.

In the experiments reported here, cesium iodide cluster anions were produced by operating the inert gas condensation portion of the source under two different sets of source conditions. In both source condition modes, cesium iodide salt (99.99%, Aldrich) was first thoroughly outgassed at 500 K, and then evaporated from a resistively heated stainless steel crucible.[41,42] The vapor was quenched in helium (99.99%) at 273 K in a condensation cell fitted with a 1.5 mm aperture. In one source condition mode (source mode 1), the crucible was maintained at a temperature of 1090 K, corresponding to a cesium iodide equilibrium vapor pressure of $\sim$2 Torr,[43] and the condensation cell pressure was maintained at approximately 10 Torr. In the other source condition mode used here (source mode 2), the crucible was heated with 1.25 times the power used in source mode 1. This resulted in a crucible temperature of 1170 K, corresponding to a cesium iodide equilibrium vapor pressure of $\sim$10 Torr. The condensation cell pressure in this case was approximately 5.5 Torr.

The cesium iodide cluster anion size distributions generated in both modes of operation appeared to be similar, consisting mostly of large cluster anions. Although the fully ionic cluster anions, $X^-(MX)_n$, have been found to be the most readily generated alkali halide cluster anions in both ion bombardment[5–10] and laser vaporization environments,[3,4,13] and they may well be formed in our source, they are not of concern in these experiments. Visible photons cannot photodetach electrons from fully ionic alkali halide cluster anions since this process would amount to the removal of an electron from an atomic iodine anion within the nanocrystal. The energy required for this process falls between the electron affinity of the iodine atom, 3.06 eV,[44] and the photon energy required to remove an electron from the valence band (iodine p band) of bulk CsI into vacuum,

6.4 eV.[45–47] The energy to photodetach $I^-(CsI)_{13}$ has been bracketed between 5.0 and 6.4 eV in photon energy studies by Whetten and co-workers.[48]

The negatively charged cesium iodide nanocrystals of interest in the present study do photodetach at visible wavelengths, with the sizes of their photodetachment signals suggesting that the dominant anions generated in this source are not fully ionic species. Probably, any species not photodetaching at visible wavelengths [e.g., $I^-(CsI)_n$] account for only a minor portion of the total ion beam intensity. The predominant species produced here possess excess electrons not associated with I^- ions in the nanocrystals, and thus have loosely bound excess electrons, corresponding either to $(CsI)_n^-$ or $Cs_m(CsI)_n^-$.

Even though $(MX)_n^-$ is not the lowest energy form for an anionic alkali halide nanocrystal, the preferential generation of stoichiometric cluster anions via inert gas condensation is easy to understand. Before it is quenched, the cesium iodide vapor is known to be comprised primarily of CsI molecules, along with substantially smaller amounts of $(CsI)_2$, $(CsI)_3$, and $(CsI)_4$.[38,43] Since this vapor will not contain atomic species from dissociation (at the crucible temperatures employed in this work), the neutral clusters from its condensation are likely to be stoichiometric in CsI. This is supported by the results of electron impact mass spectrometric studies by Pflaum, Sattler, and Recknagel[38] on cesium iodide clusters produced from inert gas condensation. Their study showed that nearly all cations produced were stoichiometric cluster ions, $(CsI)_n^+$, when low energy electrons (<10 eV) were used for ionization.

In the present study, mass spectra recorded in source mode 1 revealed intense beams of large cluster anions ($n \geqslant 25$) having lognormal intensity distributions reflecting the homogeneous nucleation conditions in the condensation cell.[49] Three smaller cluster anions, $I^-(CsI)_{12}$, $(CsI)_{13}^-$, and $I^-(CsI)_{13}$, were generated under a narrow range of source conditions which were intermediate between source modes 1 and 2, and which utilized a larger than typical cathode bias voltage (-110 V). The nonstoichiometric species were determined to be fully ionic cluster anions [rather than the corresponding $Cs(CsI)_n^-$ species of similar mass] since they did not photodetach at visible photon energies. Mass spectra recorded in source mode 2 appeared similar to those of source mode 1, but also included I^- peaks (at $\sim$5%–10% of the currents for cesium iodide cluster anions) which were found to grow with increasing crucible temperature.

The above information suggests that the negatively charged cesium iodide nanocrystals generated in source mode 1 were primarily the stoichiometric cluster anions, $(CsI)_n^-$, while in source mode 2 the stoichiometric cluster anions were accompanied by the nonstoichiometric species, $Cs_m(CsI)_n^-$. The presence of I^- in the source mode 2 mass spectra probably indicates that I atoms had dissociated from some of the nanocrystal anions and were subsequently converted to I^- via electron attachment. This would have occurred by means of a nonevaporative mechanism, most likely during negative ion formation, since thermal evaporation of cesium iodide at the modest crucible temperatures utilized should not have yielded atomic species.

Nonthermal loss of halogen atoms is known to occur in bulk metal halide systems from exposure to ultraviolet photons or to energetic electrons.[50] In cluster systems, Whetten and co-workers[48] have observed photon-stimulated ejection of halogen atoms from charged alkali halide nanocrystals. In addition, Recknagel and co-workers[12] addressed this issue in electron impact studies on sodium halide clusters produced via inert gas condensation. In their study, the dominant species in the cation mass spectra changed from the fully ionic $Na^+(NaX)_n$ species to the stoichiometric species, $(NaX)_n^+$, upon decreasing the temperature of the quench gas (using 13 eV electrons for ionization in both cases). Since the thermal evaporation of alkali halide salts at the temperatures typically employed in inert gas condensation is known to yield only intact alkali halide molecules and some small molecular clusters,[43] the results of Recknagel and co-workers indicate that even though the loss of neutral halogen atoms is a nonthermal process, it is nevertheless dependent on the cluster internal temperature prior to ionization. This result is consistent with the observations reported here. Although similar supersaturation conditions were achieved in both modes in the present experiments, the clusters produced in source mode 2 were formed using higher crucible temperatures and lower condensation cell pressures than those used in source mode 1. Thus, clusters produced in source mode 2 should have had higher internal temperatures prior to their ionization. This is consistent with the appearance of I^- in the source mode 2 mass spectra and not in the source mode 1 mass spectra. The loss of iodine by some of the cluster anions produced in source mode 2 resulted in their having excess Cs atoms, resulting in more than one excess electron in these anions.

To summarize, the above evidence suggests that stoichiometric cluster anions, $(CsI)_n^-$, were generated in source mode 1, while stoichiometric cluster anions as well as nonstoichiometric cluster anions, $Cs_m(CsI)_n^-$, were generated in source mode 2. It is interesting to note that the other ion source which has been shown to easily generate both $(MX)_n^-$ and $M(MX)_n^-$ species [along with $X^-(MX)_n$] is the flowing afterglow source employed by Miller and Lineberger[28] which is also based on the thermal evaporation of alkali halide salt.

The cesium iodide cluster anion beams observed during these experiments were often very intense. Ion currents of 110 pA were measured for $(CsI)_{60}^-$ in a Faraday cup located downstream of the ion–photon interaction region (>2 m from the source). This corresponds to a steady-state number density of nearly 10^5 ions cm^{-3}. To further gauge these intensities, it is instructive to compare them to the maximum ion currents expected under space-charge limited conditions. The space-charge limited current (in amperes) for a cylindrically symmetric charged particle beam is given by the following expression:[51,52]

$$I_{sc} = 0.9 \times 10^{-6} \frac{N^{1/2} V_a^{3/2} D^2}{M^{1/2} L^2} \tag{1}$$

in which N is the ion charge state, V_a is the accelerating voltage (in volts), M is the ion mass (in amu), D is the nominal beam diameter, and L is the distance over which the

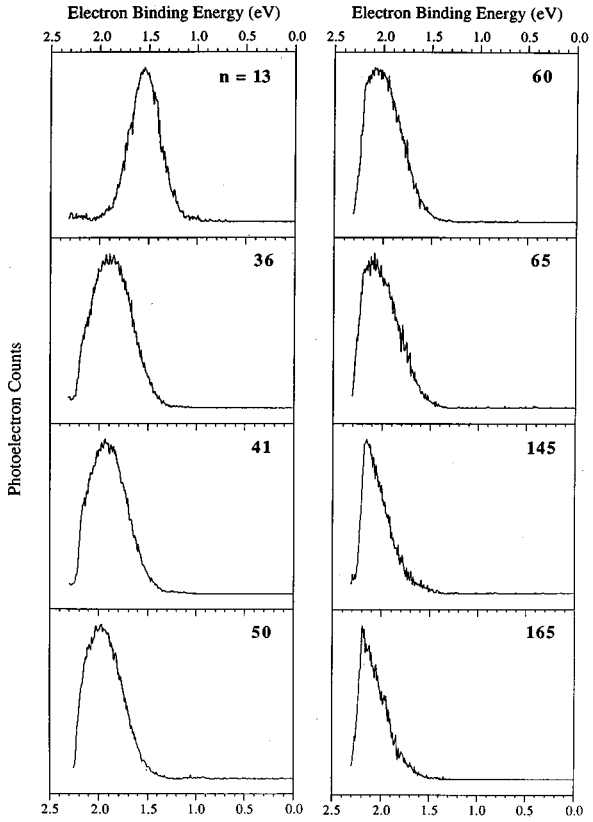

FIG. 1. Photoelectron spectra of $(CsI)_{13}^-$ and negatively charged cesium iodide nanocrystals containing 36–165 CsI units, recorded using 2.540 eV photons. $(CsI)_{13}^-$ was generated using source conditions intermediate between source modes 1 and 2. The condensation cell in the inert gas condensation ion source was operated in source mode 1 during the recording of the $n=36-165$ spectra (n=number of CsI units). For species larger than $n=36$, the spectral features are attenuated at high EBEs due to the transmission function of the electron energy analyzer.

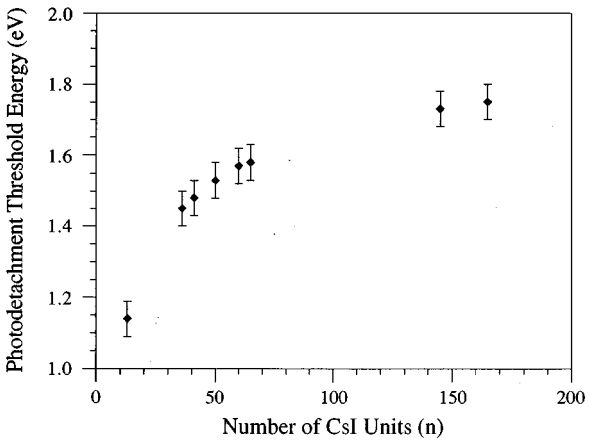

FIG. 2. Photodetachment threshold energies (ϵ_{Th}) of $(CsI)_{n=13-165}^-$ plotted vs n, the number of CsI units.

beam is transported. Since the formation of doubly charged negative ions (even at large cluster sizes) is unlikely in the present ion source environment, $N=1$ was assumed. Experimental conditions included an accelerating voltage, V_a, of 500 V, a transport distance of 2.25 m, and a nominal beam diameter of 8 mm. This diameter is chosen to correspond to the average diameter of the ion beam determined from an ion optical ray trace of our apparatus, given that the ion beam's spatial cross section expands and contracts during transport and focusing. The space-charge limited ion current for $(CsI)_{60}^-$ (15 600 amu) predicted from the above expression is 1150 pA. The observed $(CsI)_{60}^-$ current constitutes nearly 10% of the space-charge limited value, suggesting that the ion beams produced in this work were beginning to approach space-charge limited conditions.

IV. PHOTOELECTRON SPECTRA AND INTERPRETATION

All of the photoelectron spectra reported here were recorded using 2.540 eV photons. The photoelectron spectra of the stoichiometric species, $(CsI)_{n=13-165}^-$, are presented in Fig. 1. The smallest of these species, $(CsI)_{n=13}^-$, was generated using source conditions intermediate between those of source mode 1 and source mode 2, while the larger anions were generated in source mode 1. The photoelectron spectra shown in Fig. 1 are similar for all cluster anions, $n=13-165$, each consisting of a single feature which shifts to successively higher electron binding energies (EBE) with increasing cluster size. The low EBE onset in each spectrum is the photodetachment threshold energy (ϵ_{Th}) for that given cluster anion. Values for the photodetachment threshold energies, ϵ_{Th}'s, for these cesium iodide cluster anions were determined from linear extrapolations of the low EBE sides of the features in their photoelectron spectra, shown in Fig. 1. The ϵ_{Th}'s for $(CsI)_{n=13-165}^-$ are shown in Fig. 2 plotted versus n, where n represents the number of CsI units in the cluster anion. The ϵ_{Th}'s for these anions increase smoothly from 1.14 eV for $n=13$ to 1.75 eV for $n=165$. Initially, the ϵ_{Th} values rise rapidly with increasing cluster size and then appear to approach an asymptotic limit. In order to correlate the electron binding energies in these negatively charged cesium iodide nanocrystals with an excess electron binding mechanism found in extended ionic solids, it is necessary to evaluate the asymptotic limit of the photodetachment threshold energies.

The size-dependent evolution of electron binding energies (ionization potentials or electron affinities) for finite-sized metal and dielectric clusters has been evaluated using classical electrostatic models.[53–57] The observed size dependencies of cluster electron binding energies are generally in very good agreement (apart from rather small cluster sizes) with classical models which predict that electron binding energies will increase linearly toward the corresponding bulk energy value as a function of R^{-1}, where R is the radius of a spherical cluster. The specific details of nanocrystal geometries are not taken into account in this model in order to display the essentials of this physical behavior. Examining the variation of ϵ_{Th} with R^{-1} is accomplished by plotting $\epsilon_{Th}(n)$ vs $n^{-1/3}$, where the number of CsI units in the cluster, n, is related to the spherical cluster radius by $R=r_s n^{1/3}$ (where r_s is the effective radius of a single CsI pair). Plotting

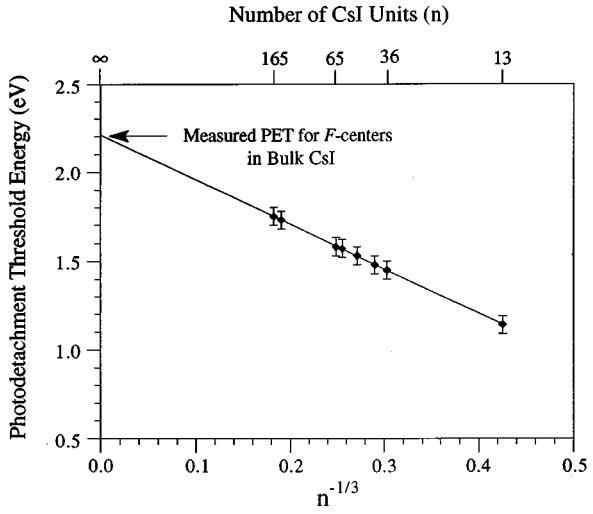

FIG. 3. Photodetachment threshold energies (ϵ_{Th}) of $(\mathrm{CsI})^-_{n=13-165}$ plotted vs $n^{-1/3}$, where n is the number of CsI units. The line drawn through the data points represents a linear least-squares fit to the experimental data.

the data in this manner clearly illustrates the asymptotic behavior of the photodetachment threshold energies, as the intercept of this plot represents the ϵ_{Th} at infinite cluster size. This essentially corresponds to the bulk crystalline photoelectric threshold corresponding to the mechanism of excess electron localization in the cluster anions.

A plot of cesium iodide cluster anion ϵ_{Th} values versus $n^{-1/3}$ is presented in Fig. 3. The ϵ_{Th} values for all these cesium iodide cluster anions, $n=13$–165, plot linearly with $n^{-1/3}$, giving a very good straight line extrapolating to a bulk $\epsilon_{\mathrm{Th}}(n=\infty)$ value of 2.2 eV. This energy corresponds to the 2.2 eV photoelectric threshold measured by Philipp and Taft for F centers in bulk cesium iodide samples at 300 K.[47] The internal temperatures of the cluster anions were also likely to be ~300 K, given that the internal temperatures of the neutral clusters were ~273 K (see source condition discussion above). This made the comparison between our extrapolated ϵ_{Th} value and the bulk photoelectric threshold value straightforward, given that thresholds can be somewhat dependent on the temperatures at which they are measured. The linear extrapolation of the cluster anion data to the analogous bulk property implies that the electron localization in these gas-phase nanocrystals is analogous to F centers in extended alkali halide crystals. These negatively charged cesium iodide nanocrystals are thus identified as stoichiometric $(\mathrm{CsI})^-_{n=13-165}$ species containing single excess electrons in embryonic F centers, which mature with increasing cluster size toward being defect centers in bulk crystalline cesium iodide.

A model describing the cluster size dependence of vertical ionization energies in discrete dielectric clusters has been presented by Landman, Jortner, and co-workers.[58–60] Their dielectric sphere model applies to homogeneous dielectric media containing spherically symmetric charge distributions, and is therefore an appropriate model for F-center containing cluster anions. The expression relating photodetachment

TABLE I. Measured photodetachment threshold energies (ϵ_{Th}) for cesium iodide nanocrystals. $(\mathrm{CsI})^-_n$, containing embryonic F centers. All energies are in eV.

n	ϵ_{Th}
13	1.14±0.50
36	1.45±0.50
41	1.48±0.50
50	1.53±0.50
60	1.57±0.50
65	1.58±0.50
145	1.73±0.50
165	1.75±0.50

threshold energies (vertical electron binding energies) to cluster size can be written as follows:

$$\epsilon_{\mathrm{Th}}(n)=\epsilon_{\mathrm{Th}}(\infty)-\frac{e^2}{2r_s}\left(1+\frac{1}{\kappa_0}-\frac{2}{\kappa_s}\right)n^{-1/3}, \tag{2}$$

where $\epsilon_{\mathrm{Th}}(\infty)$ corresponds to the photoelectric threshold (PET) for F centers in bulk cesium iodide, r_s is the effective radius of a single CsI pair, κ_0 is the high frequency dielectric constant of bulk cesium iodide, κ_s is the static dielectric constant of bulk cesium iodide, and n is the number of CsI units. If the PET measured by Philipp and Taft (2.2 eV),[47] an r_s value obtained from the bulk density of crystalline CsI (2.84 Å),[61] and the literature values for κ_0 (3.03) and κ_s (5.65),[23] are used in Eq. (2), the resultant line is essentially the same as the best fit line of the experimentally determined photodetachment threshold energies shown in Fig. 3. In fact, the ϵ_{Th} values predicted by this equation are all within ±15 meV of the experimental values presented in Table I, with the errors given there representing the variation in $\epsilon_{\mathrm{Th}}(n)$ values obtained using our linear extrapolation procedure.

The photoelectron spectra of cesium iodide nanocrystal anions with $n\approx41$–65, generated in source mode 2, are presented in Fig. 4(a). The photoelectron spectra of the F-center cluster anions of similar size (generated in source mode 1) are also shown in Fig. 4 for comparison [see Fig. 4(b)]. The spectra for the anions produced in source mode 2 are different from those of the source mode 1 anions in that they display *two* features which shift together to successively higher EBE with increasing cluster size. The higher EBE features in the source mode 2 spectra are very similar to the features in the source mode 1 spectra (which was confirmed by deconvoluting the features in the source mode 2 spectra into two separate Gaussians), while the lower EBE features indicate that a new mechanism of excess electron binding is occurring for the species generated in source mode 2. In addition, the relative intensities of the features in a given photoelectron spectrum were found to be strongly dependent on the source crucible temperature, as is illustrated in Fig. 5 for the case of $n\approx60$. This type of temperature-dependent behavior can be interpreted to indicate either the presence of new forms of $(\mathrm{CsI})^-_{n=41-65}$ that were not produced in source mode 1, or the appearance of new nanocrystal anions with slightly different stoichiometries than those generated in source mode 1. The mass spectrometric observation of I^- during source mode 2 suggests that the species responsible

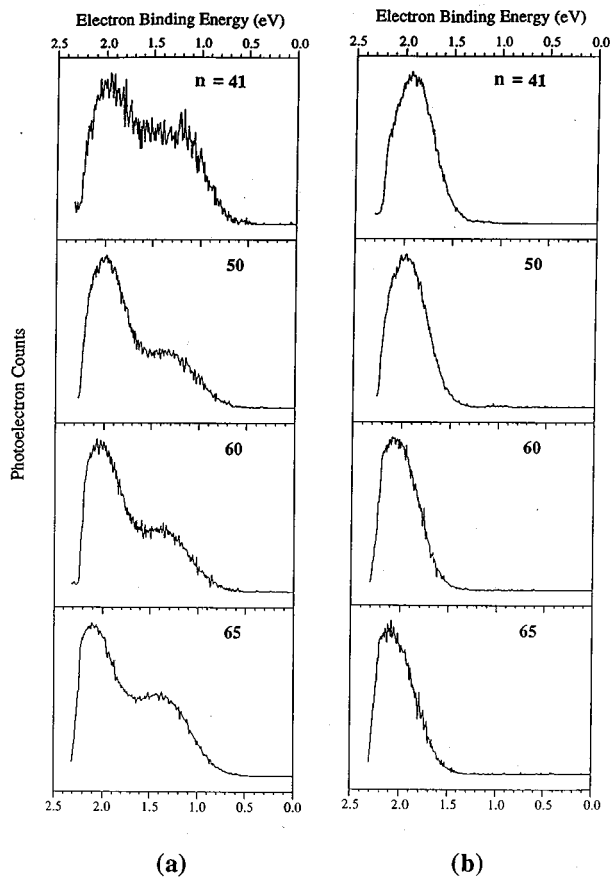

FIG. 4. Photoelectron spectra of negatively charged cesium iodide nanocrystals, $n \approx 41-65$, recorded using 2.540 eV photons. The spectra denoted (a) were recorded with the condensation cell of the inert gas condensation ion source operated in source mode 2, while the spectra denoted (b) are of the $(CsI)_n^-$ nanocrystals containing embryonic F centers (see Fig. 1).

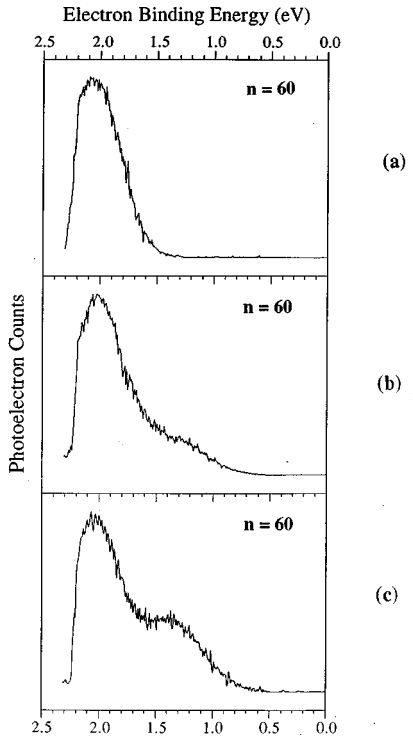

FIG. 5. Photoelectron spectra of cesium iodide nanocrystals $n \approx 60$ recorded under different source conditions using 2.540 eV photons. Spectrum (a) was recorded in source mode 1 of the ion source at the lowest crucible temperature and highest cell pressure while spectrum (c) was recorded in source mode 2 at the highest crucible temperature and lowest cell pressure. Spectrum (b) was recorded at an intermediate crucible temperature and intermediate cell pressure.

for the low EBE features in the photoelectron spectra are nonstoichiometric cesium iodide cluster anions. The cluster size dependence of the photodetachment threshold energies for the low EBE features reveals the nature of the excess electron binding in these nanocrystals.

The ϵ_{Th} values for the source mode 2 cesium iodide cluster anions were determined from linear extrapolations of the low EBE sides of the low EBE features in their photoelectron spectra. A plot of the source mode 2 cesium iodide cluster anion ϵ_{Th} values versus $n^{-1/3}$ is presented in Fig. 6, along with a plot of the $(CsI)^-_{n=13-165}$ (F center) ϵ_{Th} values versus $n^{-1/3}$. The ϵ_{Th} values for all four source mode 2 cesium iodide cluster anions, $n \approx 41-65$, also plot linearly with $n^{-1/3}$. The slope of the source mode 2 line is very similar to that for the F-center cluster anions, but extrapolates to a bulk $\epsilon_{\mathrm{Th}}(n=\infty)$ value of 1.4 eV. This energy is consistent with the PET expected for F' centers (two excess electrons in a single defect site) in bulk CsI.

Although direct measurements of the PET for F' centers in bulk CsI have not been made, this quantity can be estimated by considering either the experimentally determined PETs for F' centers in other alkali iodides or the energy band structure of cesium iodide. PETs have been measured for F' centers in KI[62] and RbI,[63] both values being 1.6 eV. The PET is expected to be a little smaller in the case of CsI since its bulk crystal has a larger lattice constant than the other iodides, and this is consistent with the extrapolated value in Fig. 6. The PET for F' centers in bulk CsI can also be estimated using the F'-center photoconductivity threshold (PCT) and the band structure of bulk CsI. The band structure of crystalline (pure) CsI is illustrated schematically in Fig. 7 with the F-center and F'-center impurity states superimposed. The PCT represents the energy required to promote an electron from a defect state to the bottom of the conduction band (i.e., the optical activation energy). For F' centers in most alkali halides, this energy is approximately 1 eV.[64] The PET is obtained by adding the PCT to the energy required to remove an electron from the bottom of the conduction band into vacuum. This latter quantity is referred to as the bulk (crystalline) electron affinity, χ (determined from the energy difference between the valence band photoemission threshold and the band gap), and for CsI, it is 0.3 eV.[45] The PET obtained from the sum of the PCT and χ is 1.3 eV, and this compares well with our extrapolated value of 1.4 eV. Thus, both methods of estimation yield numbers consistent with our extrapolated value.

The nanocrystals giving rise to the low EBE features in the source mode 2 photoelectron spectra are therefore interpreted to be embryonic F'-center containing species. We fur-

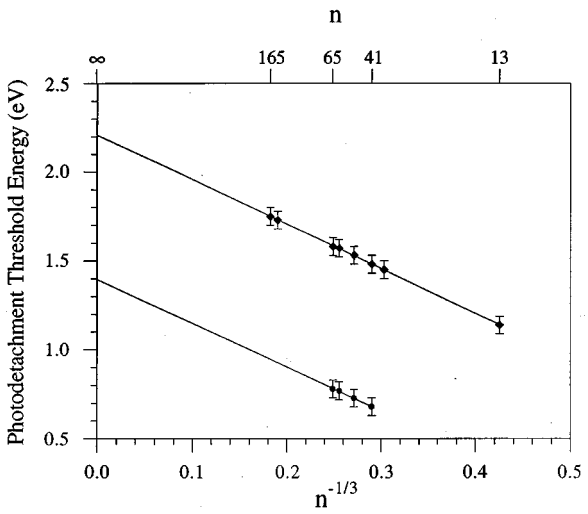

FIG. 6. Photodetachment threshold energies (ϵ_{Th}) of cesium iodide nanocrystal anions generated while operating the condensation cell in source mode 2 (●) plotted vs $n^{-1/3}$ (lower plot). The ϵ_{Th} values of the F-center containing species (♦) are also shown for comparison (upper plot). The lines drawn through each set of data points represent linear least-squares fits to the experimental data.

ther interpret these species to be cesium iodide nanocrystals having excess metal atoms, consistent with our deductions based on the ion production information for source mode 2. The most likely candidates are $Cs(CsI)_n^-$ species, cluster anions which possess two excess electrons. The ϵ_{Th} values for embryonic F' centers in these nanocrystals are presented in Table II. It is interesting to note that the formation of embryonic F' centers in cesium iodide nanocrystals in this study begins with neutral clusters whose internal temperatures are higher than those of the clusters which eventually become F-center species after negative ion formation. At first sight, this is somewhat unexpected, considering that the formation of F' centers in bulk alkali halides is usually associated with cryogenic environments.[22,62,63] The generation of embryonic F' centers here can be understood, however, by realizing that the loss of iodine will not only provide the nanocrystals with excess electrons (via extra metal atoms), but may also serve to decrease the internal energies of the nanocrystals.

TABLE II. Measured photodetachment threshold energies (ϵ_{Th}) for cesium iodide nanocrystals, $Cs(CsI)_n^-$, containing embryonic F' centers. All energies are in eV.

n	ϵ_{Th}
41	0.68±0.50
50	0.73±0.50
60	0.77±0.50
65	0.78±0.50

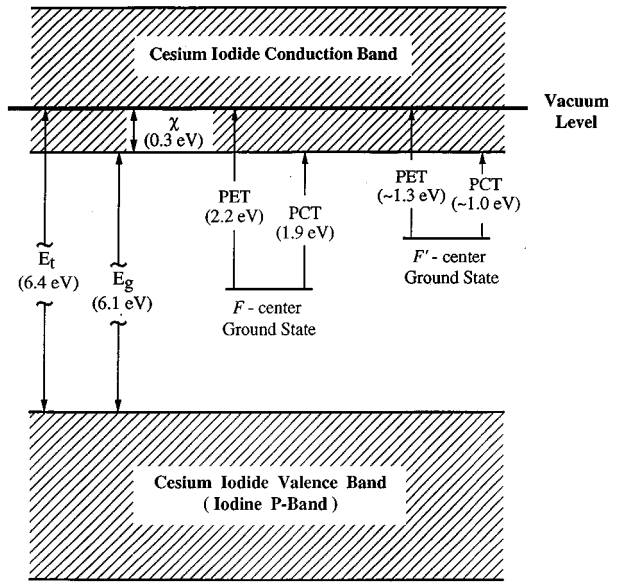

FIG. 7. Illustration of the electronic band structure of bulk crystalline cesium iodide showing vertical energy relationships. The ground state energy levels for the F-center and F'-center impurity states are also represented. On this figure, E_t=the valence band photoemission threshold, E_g=the band gap energy, χ=the crystalline electron affinity, PET=impurity center photoelectric threshold, PCT=impurity center photoconductivity threshold (or optical activation energy).

In our analysis of the source mode 2 photoelectron spectra, we considered several alternative explanations for the presence of the low EBE features, but none was found to be satisfactory. For example, embryonic F' centers might exist within doubly charged stoichiometric cluster anions, $(CsI)_n^=$, but available evidence suggests that such species were not produced in these experiments. If $(CsI)_n^=$ had been produced and then given rise to the low EBE features in the source mode 2 photoelectron spectra, analogous features would probably have appeared in the source mode 1 spectra as well. Since the cluster formation and ionization regions of the ion source are largely separate, the intensities of low EBE features arising from doubly charged anions would depend on the source conditions relevant to ion formation rather than on crucible temperature, as was actually observed. In addition, the ion source conditions most relevant to ion formation (i.e., the cathode bias and emission current) were the same for both modes. Another explanation we considered for the low EBE features was that they resulted from the photodetachment of electronically excited F centers in stoichiometric cesium iodide cluster anions. It is unlikely, however, that such species would have been present in the ion–photon interaction region, since luminescence to the F-center electronic ground state in bulk cesium iodide occurs on a time scale over 10 times faster than the ion transit time in our apparatus.[65] This possibility also seems unlikely on the basis of energetics. The energy required to promote an electron from an excited state F center into the conduction band of bulk cesium iodide is 0.052 eV.[66] The PET for excited state F centers in bulk cesium iodide is therefore expected to be only 0.352 eV, which is inconsistent with the extrapolated ϵ_{Th} value for the low EBE features. The possibility that the low EBE features might have resulted from the photodetachment of electrons loosely bound in the lowest unoccupied molecular orbitals (LUMOs) of closed-shell cesium iodide nanocrystals was also considered. Since the unoccupied orbitals of the clusters will eventually develop into the conduc-

tion band of the bulk as cluster size increases, the upper limit to the binding energy in this case would be the crystalline electron affinity, χ. As stated, this quantity is 0.3 eV for cesium iodide. This energy is again inconsistent with our extrapolated ϵ_{Th} value for the low EBE features, which points to stronger electron binding.

Having ascribed the low EBE features in the source mode 2 photoelectron spectra to embryonic F' centers in $\mathrm{Cs(CsI)}_n^-$, the origin of the high EBE features is now considered. As mentioned, the high EBE features are very similar (if not identical) to the features in the source mode 1 spectra, implying that they result from the photodetachment of electrons from embryonic F-center environments. These high EBE features can therefore be attributed to photodetachment from one of two separate F centers within a given $\mathrm{Cs(CsI)}_n^-$ cluster anion, to spectral contributions from adjacent-sized stoichiometric cluster anions, or to both. In cluster anions of the sizes considered here, F centers in different nanocrystal sites are likely to have similar photodetachment threshold energies, in contrast with small cluster anions ($n \leqslant 13$) where different binding sites are more likely to have dissimilar local environments.[32,33] The interpretation presented above satisfactorily accounts for all of the observed features in the cesium iodide cluster anion photoelectron spectra.

Last, it should be noted that multiple excess electron binding in the form of tightly bound spin pairs in M^- sites [for $\mathrm{K(KI)}_{n\leqslant 21}^-$ and $\mathrm{Na(NaCl)}_{n\leqslant 21}^-$] has also been reported.[29,32,33] If such binding also occurs in the case of cesium iodide cluster anions, the relevant photoelectron features are either out of our spectral range or obscured by the main features discussed above.

V. DISCUSSION

The success of the dielectric sphere model in predicting the F-center CsI nanocrystal ϵ_{Th} (photodetachment threshold energy) values suggests the further application of such models to estimate additional properties of defect state alkali halide nanocrystals. Before we proceed, however, several aspects of this model pertaining to cesium iodide cluster anions in particular should be discussed. The ability of this simple model to so closely predict the F-center CsI nanocrystal ϵ_{Th} values is at first sight surprising, since the cesium iodide nanocrystal structures are likely to be rocksaltlike, while the bulk crystal structure of CsI is bcc rather than fcc. Li and Whetten have considered the structure of fcc cesium iodide based on ionic radii and found that the fcc lattice constant would be close to the actual bcc constant.[15] In light of this, it is reasonable to assume that the densities and dielectric properties of fcc and bcc CsI would be similar, and this may partially account for the match between the energies predicted by the model and the observed ϵ_{Th} values.

The ability of the dielectric sphere model to predict the ϵ_{Th} of $(\mathrm{CsI})_{13}^-$ is also somewhat intriguing. The $(\mathrm{MX})_{13}^-$ species are expected to have $3\times3\times3$ arrangements analogous to the $X^-(\mathrm{MX})_{13}$ nanocrystals, but with the excess electron taking the place of a corner halogen anion,[4,29,31] i.e., $(\mathrm{CsI})_{13}^-$ is expected to possess a localized surface F center. Since the dielectric sphere model given above applies strictly to localized excess charge distributions internalized in homogeneous dielectric clusters, it is not immediately apparent that surface-localized electrons would be adequately described by the model. This situation was recently examined in a theoretical study by Makov and Nitzan,[67] who developed a model that specifically applies to the ionization of localized charges ''solvated'' at dielectric cluster surfaces. Their model not only predicts an $n^{-1/3}$ (i.e., R^{-1}) dependence, just as the sphere model described above, but further predicts the slope of the $n^{-1/3}$ line to be insensitive to the actual location of the excess charge. Thus, the adherence of the ϵ_{Th} value of $(\mathrm{CsI})_{13}^-$ to the dielectric sphere line simply indicates that this anion possesses an embryonic F center, regardless of the particular position of the localized excess electron.

With this result in hand, we then used the dielectric sphere model with the measured PET of F centers in KI,[62,69] the dielectric constants of KI,[23] and an r_s value from the bulk density of KI[61] to predict the ϵ_{Th} of $(\mathrm{KI})_{13}^-$ which has been measured by Bloomfield and Smalley.[29] This method predicts an ϵ_{Th} value of 1.53 eV, in very good agreement with the threshold in their experimental spectrum, lending additional support to their interpretation of this anion as an F-center species. On the strength of the model in predicting the ϵ_{Th} values for both $(\mathrm{CsI})_{13}^-$ and $(\mathrm{KI})_{13}^-$, we went on to apply this model to estimate F-center ϵ_{Th} values in cluster anions of other alkali halides. The PETs for F centers in several bulk alkali halides (KI, RbI, and CsI)[47,62,68–70] have been measured, and PET values for F centers in other bulk alkali halides can be estimated in the following manner. The ratio of the experimentally determined PET for F centers in KI[62] to that for F centers in RbI[70] can be very accurately predicted by taking the ratio of the magnitudes of the total energies for these F centers, calculated using a point-ion model with ion-size corrections.[64] Using this correlation, the PET for F centers in a given alkali halide can be estimated by scaling the PET value measured for F centers in KI by the ratio of the computed total energy for F centers in that alkali halide to that for F centers in KI.

The case of NaCl is first examined since experiments have been carried out on $\mathrm{(NaCl)}_{n\leqslant 22}^-$ by Bloomfield and co-workers[31] who interpreted both the $n=13$ and $n=22$ cluster anions to be F-center species ($3\times3\times3$ and $3\times3\times5$, respectively) in which the excess electrons reside in corner anion vacancies. Using the above procedure, the scaled PET for F centers in bulk NaCl is found to be 2.96 eV. Using this PET and the other constants for bulk NaCl in the dielectric sphere model, the ϵ_{Th} for $(\mathrm{NaCl})_{13}^-$ is estimated to be 1.45 eV, while the ϵ_{Th} for $(\mathrm{NaCl})_{22}^-$ is estimated to be 1.69 eV. Both estimates are in very good agreement with the observed thresholds in the photoelectron spectra, and again add support to the interpretation of these cluster anions as F-center species. The repeated success of this approach suggests that the ϵ_{Th}'s of other $(\mathrm{MX})_{13}^-$ F-center species can be estimated in an analogous fashion. The ϵ_{Th} values for the $(\mathrm{MX})_{13}^-$ species for a variety of alkali halides estimated from the dielectric cluster model using bulk dielectric constants and scaled bulk F-center PET's are given in Table III.

A dielectric sphere model approach can also be used to estimate the adiabatic electron affinities of cesium iodide clusters containing defect centers. The term electron affinity

TABLE III. Estimated (predicted) photodetachment threshold energies (ϵ_{Th}) for embryonic F centers in $(MX)_{13}^-$ nanocrystals calculated using the dielectric sphere model. All energies in eV.

MX	ϵ_{Th}
LiF	0.96
LiCl	1.30
LiBr	1.36
LiI	1.43
NaF	1.30
NaCl	1.45
NaBr	1.50
NaI	1.44
KF	1.61
KCl	1.57
KBr	1.57
KI	1.53
RbF	1.91
RbCl	1.64
RbBr	1.59
RbI	1.53
CsI	1.15

is used here to describe the adiabatic binding energies of electrons in defect (impurity) state cluster anions, which is different from its previous use to describe the electron binding energy of the pure crystalline solid, χ. In addition, it should be noted that the adiabatic electron affinities of cesium iodide cluster anions should not necessarily correspond to their ϵ_{Th} values, as the latter are determined by vertical energy relationships. The dielectric sphere model equation for adiabatic electron affinities (accompanying the vertical expression presented above) is[58–60]

$$\mathrm{EA}(n)=\mathrm{EA}(\infty)-\frac{e^2}{2r_s}\left(1-\frac{1}{\kappa_s}\right)n^{-1/3}, \tag{3}$$

where EA(∞) corresponds to the threshold for the thermionic emission of electrons from F centers in bulk CsI. Since no measurements of this quantity are available, this quantity must be estimated. The bulk thermionic emission threshold (TET) can be estimated using a simple impurity center cavity model[23] and the bulk PET value. In this model for ionic crystals, the PET$\sim e^2/2\kappa_0 R_c$, while the TET$\sim e^2/2\kappa_s R_c$, (where R_c is taken to be the cavity radius of the impurity center). The ratio of κ_s to κ_0 thus gives the ratio of the TET to the PET. The derived TET is 1.2 eV, and when used in the dielectric model, the electron affinities of the neutral $(CsI)_n$ counterparts to the F-center cluster anions are estimated to range from $\sim$0.3 eV for $n=13$ to $\sim$0.8 eV for $n=165$.

We now turn our attention to the F'-center containing cesium iodide nanocrystal anions. The electron affinities of the F'-center containing nanocrystals can be examined in a manner analogous to that for the F-center nanocrystals. The TET for F' centers in CsI is roughly estimated to be 0.7 eV using the ratio of the dielectric constants and the PET for F' centers in CsI. Using this value in the EA dielectric sphere equation,[71] it is predicted that the electron affinities will first become positive around $n=25$ CsI units, suggesting that below this size, F' centers in CsI nanocrystals are not stable. Theoretical calculations by Landman on the analogous system of dielectrons in water clusters[72] find that clusters with two electrons localized in single cavities strongly prefer to have the charges internalized within the dielectric environment of the cluster. In light of this, perhaps the F' centers in cesium iodide nanocrystals (becoming stable at $n\sim25$) are internalized. In some sense, this cluster size may also represent the point at which F centers can become internalized, since they can be viewed as ''trapping sites'' for second electrons in the F'-center formation process.

In conclusion, it should be noted that the results of the present study are consistent both with the results of previous photoelectron experiments on smaller alkali halide cluster anions and with the theoretical predictions of Landman, Scharf, and Jortner,[17] who first postulated that excess electron localization in small alkali halide clusters could be manifested as physically similar entities to those seen in extended ionic solids.

VI. SUMMARY

The photoelectron spectra of negatively charged cesium iodide nanocrystals, recorded using 2.540 eV photons, are presented. Excess electron nanocrystals comprised of 26 to 330 atoms are examined. Depending on their formation conditions, these nanocrystals show two distinct types of photoemission behavior which indicate different modes of excess electron localization. The correlation of the observed photoemission behavior to bulk behavior provides evidence for the existence of embryonic F centers and embryonic F' centers in negatively charged cesium iodide nanocrystals. Stoichiometric cluster anions, $(CsI)_n^-$, containing single excess electrons can localize them in embryonic F centers, while cluster anions with two excess electrons, $Cs(CsI)_n^-$, are capable of localizing these electrons together in single defect sites as embryonic F' centers, or separately in two embryonic F-center defects in the same cluster anion.

ACKNOWLEDGMENTS

We wish to thank U. Landman and R. L. Whetten for many helpful discussions and also thank L. A. Bloomfield, P. E. Cade, J. V. Coe, R. N. Compton, S. N. Khanna, and I. Schneider for productive discussions. We gratefully acknowledge the support of the National Science Foundation under Grant No. CHE-9007445.

[1] T. P. Martin, Phys. Rep. **95**, 167 (1983).
[2] R. L. Whetten, Acc. Chem. Res. **26**, 49 (1993).
[3] E. C. Honea, M. L. Homer, and R. L. Whetten, Int. J. Mass Spectrom. Ion Proc. **102**, 213 (1990).
[4] L. A. Bloomfield, C. W. S. Conover, Y. A. Yang, Y. J. Twu, and N. G. Phillips, Z. Phys. D: Atoms, Mol. Clusters **20**, 93 (1991).
[5] F. Honda, G. M. Lancaster, Y. Fukuda, and J. W. Rabalais, J. Chem. Phys. **69**, 4931 (1978).
[6] J. E. Campana, T. M. Barlak, R. J. Colton, J. J. DeCorpo, J. R. Wyatt, and B. I. Dunlap, Phys. Rev. Lett. **47**, 1046 (1981); T. M. Barlak, J. E. Campana, R. J. Colton, J. J. DeCorpo, and J. R. Wyatt, J. Phys. Chem. **85**, 3840 (1981); T. M. Barlak, J. R. Wyatt, R. J. Colton, J. J. DeCorpo, and J. E. Campana, J. Am. Chem. Soc. **104**, 1212 (1982); T. M. Barlak, J. E. Campana, J. R. Wyatt, B. I. Dunlap, and R. J. Colton, Int. J. Mass Spectrom. Ion Proc. **46**, 523 (1983); J. E. Campana, R. J. Colton, J. R. Wyatt, R. H. Bateman, and B. N. Green, Appl. Spectrosc. **38**, 430 (1984).
[7] W. Ens, R. Beavis, and K. G. Standing, Phys. Rev. Lett. **50**, 27 (1983).

[8] M. A. Baldwin, C. J. Proctor, I. J. Amster, and F. W. McLafferty, Int. J. Mass Spectrom. Ion Proc. **54**, 97 (1983).
[9] I. Katakuse, H. Nakabushi, T. Ichihara, T. Sakurai, T. Matsuo, and H. Matsuda, Int. J. Mass Spectrom. Ion. Proc. **57**, 239 (1984); **62**, 17 (1984).
[10] H. J. Hwang, D. K. Sensharma, and M. A. El-Sayed, Phys. Rev. Lett. **64**, 808 (1990).
[11] T. P. Martin, Ber. Bunsenges. Phys. Chem. **88**, 300 (1984).
[12] R. Pflaum, P. Pfau, K. Sattler, and E. Recknagel, Surf. Sci. **156**, 165 (1985).
[13] Y. J. Twu, C. W. S. Conover, Y. A. Yang, and L. A. Bloomfield, Phys. Rev. B **42**, 5306 (1990).
[14] M. L. Homer, F. E. Livingston, and R. L. Whetten, J. Am. Chem. Soc. **114**, 6558 (1992); Z. Phys. D: Atoms, Mol., Clusters **26**, 201 (1993).
[15] X. Li and R. L. Whetten, J. Chem. Phys. **98**, 6170 (1993).
[16] J. P. Rose and R. S. Berry, J. Chem. Phys. **96**, 517 (1992); Z. Phys. D: Atoms, Mol., Clusters **26**, 189 (1993).
[17] U. Landman, D. Scharf, and J. Jortner, Phys. Rev. Lett. **54**, 1860 (1985).
[18] D. Scharf, J. Jortner, and U. Landman, J. Chem. Phys. **87**, 2716 (1987).
[19] K. K. Sunil and K. D. Jordan, J. Phys. Chem. **91**, 1710 (1987).
[20] R. N. Barnett, U. Landman, D. Scharf, and J. Jortner, Acc. Chem. Res. **22**, 350 (1989).
[21] G. Rajagopal, R. N. Barnett, and U. Landman, Phys. Rev. Lett. **67**, 727 (1991); U. Landman, R. N. Barnett, C. L. Cleveland, and G. Rajagopal, NATO ASI Series C **374**, 165 (1992).
[22] F. Seitz, Rev. Mod. Phys. **18**, 384 (1946); **26**, 7 (1954).
[23] N. F. Mott and R. W. Gurney, *Electronic Processes in Ionic Crystals* (Clarendon, Oxford, 1948).
[24] J. H. Schulman and W. D. Compton, *Color Centers in Solids* (Pergamon, New York, 1962).
[25] *Physics of Color Centers*, edited by W. B. Fowler (Academic, New York, 1968).
[26] E. C. Honea, M. L. Homer, P. Labastie, and R. L. Whetten, Phys. Rev. Lett. **63**, 394 (1989).
[27] G. Rajagopal, R. N. Barnett, A. Nitzan, U. Landman, E. C. Honea, P. Labastie, M. L. Homer, and R. L. Whetten, Phys. Rev. Lett. **64**, 2933 (1990).
[28] T. M. Miller and W. C. Lineberger, Int. J. Mass Spectrom. Ion Proc. **102**, 239 (1990).
[29] Y. A. Yang, L. A. Bloomfield, C. Jin, L. S. Wang, and R. E. Smalley, J. Chem. Phys. **96**, 2453 (1992).
[30] Y. A. Yang, C. W. S. Conover, and L. A. Bloomfield, Chem. Phys. Lett. **158**, 279 (1989).
[31] P. Xia, A. J. Cox, Y. A. Yang, and L. A. Bloomfield, NATO ASI Series C **374**, 1019 (1992).
[32] P. Xia, A. J. Cox, and L. A. Bloomfield, Z. Phys. D: Atoms, Mol., Clusters **26**, 184 (1993).
[33] P. Xia and L. A. Bloomfield, Phys. Rev. Lett. **70**, 1779 (1993).
[34] J. V. Coe, J. T. Snodgrass, C. B. Freidhoff, K. M. McHugh, and K. H. Bowen, J. Chem. Phys. **84**, 618 (1986).
[35] H. W. Sarkas, L. H. Kidder, J. G. Eaton, K. M. McHugh, and K. H. Bowen, Mater. Res. Soc. Symp. Proc. **206**, 277 (1991).
[36] T. P. Martin, J. Chem. Phys. **81**, 4426 (1984).
[37] J. Diefenbach and T. P. Martin, J. Chem. Phys. **83**, 2238 (1985).
[38] R. Pflaum, K. Sattler, and E. Recknagel, Phys. Rev. B **33**, 1522 (1986).
[39] A. T. Forrester, *Large Ion Beams: Fundamentals of Generation and Propagation* (Wiley, New York, 1988).
[40] I. Langmuir, Phys. Rev. **26**, 585 (1925).
[41] H. J. Loesch and D. R. Herschbach, J. Chem. Phys. **57**, 2038 (1972).
[42] E. F. Greene, in *Alkali Halide Vapors*, edited by P. Davidovits and D. L. McFadden (Academic, New York, 1979), p. 33.
[43] M. S. Chandrasekharaiah, in *The Characterization of High Temperature Vapors*, edited by J. L. Margrave (Wiley, New York, 1967), p. 495.
[44] H. Hotop and W. C. Lineberger, J. Phys. Chem. Ref. Data **14**, 731 (1985).
[45] R. T. Poole, J. G. Jenkin, J. Liesegang, and R. C. G. Leckey, Phys. Rev. B **11**, 5179 (1975).
[46] T. H. DiStefano and W. E. Spicer, Phys. Rev. B **7**, 1554 (1973).
[47] H. R. Philipp and E. A. Taft, J. Phys. Chem. Solids **1**, 159 (1956).
[48] X. Li, R. D. Beck, and R. L. Whetten, Phys. Rev. Lett. **68**, 3420 (1992).
[49] C. G. Granqvist and R. A. Buhrman, J. Appl. Phys. **47**, 2200 (1976).
[50] U. O. Karlsson, F. J. Himpsel, J. F. Morar, F. R. McFeeley, D. Rieger, and J. A. Yarmoff, Phys. Rev. Lett. **57**, 1247 (1986); C. L. Strecker, W. E. Moddeman, and J. T. Grant, J. Appl. Phys. **52**, 6921 (1981).
[51] J. R. Pierce, *Theory and Design of Electron Beams* (Van Nostrand, New York, 1954).
[52] R. Hutter, in *Focusing of Charged Particles*, edited by A. Septier (Academic, New York, 1967) Vol. 2, p. 3.
[53] J. M. Smith, AIAA J. **3**, 648 (1965).
[54] D. M. Wood, Phys. Rev. Lett. **46**, 749 (1981).
[55] L. E. Brus, J. Chem. Phys. **79**, 5566 (1983).
[56] L. E. Brus, J. Chem. Phys. **80**, 4403 (1984).
[57] G. Makov, A. Nitzan, and L. E. Brus, J. Chem. Phys. **88**, 5076 (1988).
[58] R. N. Barnett, U. Landman, C. L. Cleveland, and J. Jortner, Chem. Phys. Lett. **145**, 382 (1988).
[59] J. Jortner, U. Even, N. Ben-Horin, D. Scharf, R. N. Barnett, and U. Landman, Z. Phys. D: Atoms, Mol., Clusters **12**, 167 (1989).
[60] J. Jortner, Z. Phys. D: Atoms, Mol., Clusters **24**, 247 (1992).
[61] *CRC Handbook of Chemistry and Physics*, 74th ed., edited by D. R. Lide (Chemical Rubber, Boca Raton, FL, 1993), p. 4-52.
[62] H. R. Philipp and E. A. Taft, Phys. Rev. **106**, 671 (1957).
[63] E. Taft and L. Apker, Phys. Rev. **83**, 479 (1951).
[64] A. M. Stoneham, *Theory of Defects in Solids: Electronic Structure of Defects in Insulators and Semiconductors* (Clarendon, Oxford, 1975), p. 567.
[65] Reference 25, p. 627.
[66] D. Lynch, A. Brothers, and D. Robinson, Phys. Rev. A **139**, 285 (1965).
[67] G. Makov and A. Nitzan, J. Phys. Chem. **98**, 3459 (1994).
[68] L. Apker and E. Taft, in *Imperfections in Nearly Perfect Crystals*, edited by W. Shockley, J. H. Hollomon, R. Maurer, and F. Seitz (Wiley, New York, 1952), p. 246.
[69] L. Apker and E. Taft, Phys. Rev. **79**, 964 (1950).
[70] L. Apker and E. Taft, Phys. Rev. **81**, 698 (1951).
[71] Note that the dielectric sphere model in the form presented may not strictly apply to clusters having defect states with two charge carriers.
[72] H.-P. Kaukonen, R. N. Barnett, and U. Landman, J. Chem. Phys. **97**, 1365 (1992).